Effect of Size and Shape of PDC Cutter on Wear Rate

in Multi Layer Formation

By

Kong Kai Vern

14738

Dissertation submitted in partial fulfillment of
the requirements for the
Bachelor of Engineering (Hons)
(MECHANICAL ENGINEERING)

JANUARY 2015

Universiti Teknologi PETRONAS

32610 Bandar Seri Iskandar

Perak Darul Ridzuan

CERTIFICATION OF APPROVAL

EFFECT OF SIZE AND SHAPE OF PDC CUTTER ON WEAR RATE IN MULTI LAYER FORMATION

By

Kong Kai Vern

A project dissertation submitted to the

Mechanical Engineering Programme

Universiti Teknologi PETRONAS

in partial fulfilment of the requirement for the

BACHELOR OF ENGINEERING (Hons)

(MECHANICAL ENGINEERING)

Approved by,

____

(AP Dr Ahmad Majdi Bin Abdul Rani)

Universiti Teknologi PETRONAS

32610 Bandar Seri Iskandar,

Perak Darul Ridzuan, Malaysia.

January 2015

CERTIFICATION OF ORIGINALITY

This is to certify that I am responsible for the work submitted in this project, that the original work is my own except as specified in the references and acknowledgements, and that the original work contained herein have not been undertaken or done by unspecified sources or persons.

____

Kong Kai Vern

ACKNOWLEDGEMENT

An endeavour over a period can be successful only with the advice and support of well-wishers. The author would like to take this opportunity to express his profound gratitude to Universiti Teknologi PETRONAS for providing the platform for the research project to be conducted.

The author also take this opportunity to express a deep sense of gratitude and regards to his supervisor, **AP Dr Ahmad Majdi Abdul Rani**, Senior Lecturer, Mechanical Engineering, Universiti Teknologi PETRONAS, for his cordial support, valuable information and exemplary guidance, which help the author in completing the final year project. The blessing, help and guidance given by him time to time shall carry the author a long way in the journey of life on which the author about to embark.

The gratitude also goes to **Dr Shahrul Kamaruddin** and **Dr Abdul Rahim Othman** for their guidance in doing the simulation in ABAQUS software and supervision in completing the project. A big contribution and hard worked from them during project progress is very great indeed.

Last but not least, the author would like to his parents and friends for their constant encouragement without which this report would not be possible.

Abstract

During a normal drilling operation, the rate of penetration (ROP) often over focused while the wear rate is less taken care of. However, wear rate is a more severe problem faced in a long run drilling operation in multi-layer formation rather than focusing solely on the ROP. The project is to investigate the effect of Polycrystalline Diamond Compact (PDC) bit design features on the bit wear rate during the operation in multi-layer formation, which is sandstone formation and dolomite formation. The bit design features studied in the project is the shape of the cutters and the size of the cutters. The effect of drilling fluid is assumed to be optimum. Using ABAQUS, models with different shape of cutter and size of cutter are simulated and compared. Results are analyzed and compared to study the effects on wear rate and select the best model which has minimum wear rate. Result showed that 16mm size cutter and cone shape cutter are best design to minimize the cutter wear compared to other size and shape of cutter used in the project.

Table of Contents

Chapter 3: Methodology

Chapter 4: Result and Discussion

Chapter 5: Conclusion and Recommendations

List of Figures

List of Tables

Chapter 1

Introduction

1.1. Background

Drilling is an important operation in oil and gas industry. Polycrystalline Diamond Compact (PDC) bit is used often on the drilling process (FIGURE 1.1). The time taken for the drilling operation is directly proportional to the cost (Bilgesu, Tetrick, Altmis, Mohaghegh, & Ameri, 1997). However, by increasing the rate of penetration (ROP) might be able to reduce the time needed for the operation, it also reduce the lifespan of the drilling bit. Drill bit will suffer severe damage if the bit design is not suitable for the type of formation the operation is undergoing. Then, the drill bit becomes another major cost of the operation. To minimize the wear rate of the drilling bit, several parameters of the bit design are chosen to be compared.

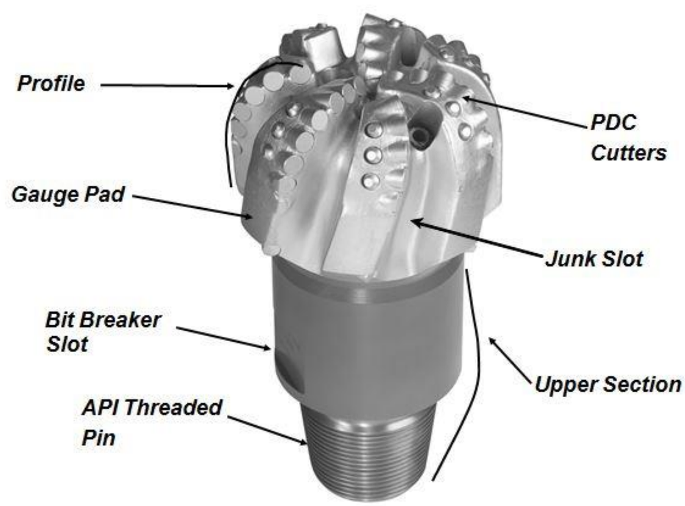

FIGURE 1.1: PDC bit

Drilling performance is influenced by the type of formation, bit hydraulics, ROP, weight on bit (WOB) and the wear rate. The project will be focusing on the effect of bit design features on the wear rate, which included size of cutter, shape of cutter, number of back-up cutter and bit material. By minimizing the wear rate, it increases the run length of the drilling operation and directly affects the time needed for the operation to cut short, resulting in the decrease in cost and optimizing the performances.

1.2. Problem Statement

During the drilling operation, ROP is commonly used for rating the drilling performance. However, as mentioned before, to reduce cost or optimize the drilling performance, maximizing the ROP is not the only way. Sometime, run length is more preferable especially in the drilling operation of multi layer formation. When the drill bit is worn out, the team will need to bring the drill bit all the way up and change it. This consumed a lot of time. Moreover, when the drill bit is worn out but the drilling operation is still carried on, the connection between the drill bit and bottom hole assembly (BHA) tools might break and the team will need to fish the broken drill bit out before the drilling operation can be continued. Another issue is, if the parts are not able to fish out, the team will need to recalculate a new route which can avoid the particular spot. In the end, all of these consumed a lot of unnecessary time. This project is to assist in this problem by obtaining a bit design which allow minimal wear rate to occur by altering the size and shape of the cutters. Thus, preventing the lost of time and increase the run length of the drill bit.

1.3. Objectives

This research is to study how the PDC bit can be worn during the process of drilling and using what size and shape of cutters are able to successfully reduce its wear rate. Different types of PDC bit design are simulated to get a relatively better design with minimum wear rate. Thus, the objectives of this research are:

- To understand the PDC cutter through analytical model.
- To simulate the effect of the size and shape of cutter on the stress distribution.
- To establish the relationship between stress and wear using wear equation.
- To determine the best size and shape of cutter for multi-layer formation.

1.4. Scope of Study

The research relates overall to compare different type of combinations of bit design to deduce a best design in minimizing the wear rate of the bit. Due to the limitation of time frame and software, the bit design used in the research limit to size and shape of the cutter. PDC bit design is chosen as this type of cutter is most commonly used in the oil and gas industry for hard formation. The drilling fluid assumed to be functioning well and effective cleaning thus can be ignored in the drilling operation. The multi-layer formation properties chosen in this project is sandstone which represents the relatively soft formation and dolomite which represents the hard formation. These two formations are chosen as they are categorized in the sedimentary rocks which are more common in the drilling operation.

Chapter 2

Literature Review

2.1. Bit Wear

During the drilling operation, the drill bit is subjected to highly abrasive rock and also the high velocity drilling fluid which will cause serious wear (FIGURE 2.1) and corrosion to the bit profile (Li & Hood, 1993). Thus, selecting a suitable bit design that is suitable for the job is very crucial.

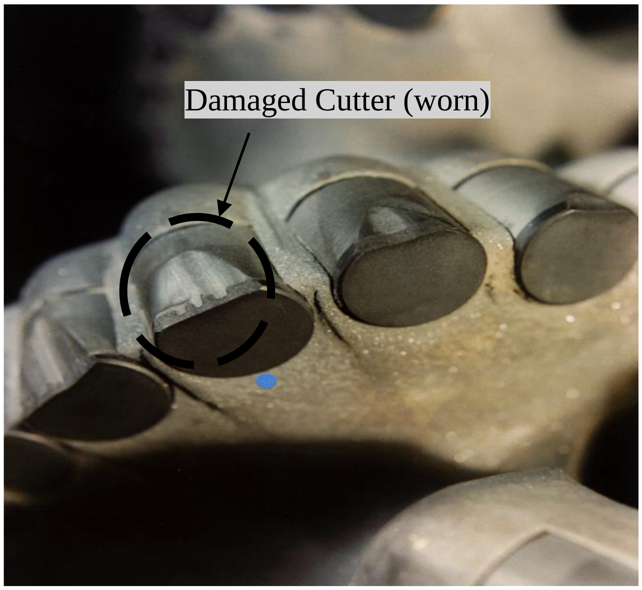

FIGURE 2.1: Common bit wear

The drilling bit is normally subjected to abrasive wear and thermal damage (Smith International Inc, 2002). Abrasive wear occurred during the impact between the bit and the rock in the formation (Henry, Corp, Sherif & Ahmed Ragheb, 2011). During the impact, the bit experience some loss as the diamond grain is crushing with the rock, causing it to gradually removed from the bit. When the worn part is gradually removed from the bit, new diamond grain is exposed to the drilling and the crushing and removing process repeat itself as the drilling operation continue.

Abrasive wear in soft formation is minimal, however, when the formation consist of hard stingers, or when the hardness of the formation increased, the wear rate become more and more severe (Yahiaoui, Gerbaud, Paris, Denape, & Dourfaye, 2012). The higher the different between the bit and the formation will cause a more severe wear rate to the bit (Cheatham & Loeb, 1985).

While for thermal damage, when the temperature continues to rise and over pass 662 Fahrenheit, the unfavorable stress condition begin to occur in the bit. When the temperature increased, the hardness of the PDC bit decreased. Research have shown that the hardness of the PDC bit decrease for more than 65% when the temperature arose near to 1300 Fahrenheit, when compared to its hardness during room temperature. This further increase the abrasive wear as the difference in hardness of the bit and the formation hardness will directly affect the wear rate of the bit (Glowka, & Stone, 1986).

2.2. Multi Layer Formation

Multi layer formation is defined as different types of formation interbedded with another types of formation (FIGURE 2.2). In multi layer formation, the hardness of the formation is always changing (Muhammad Hariz, 2014); it might change from a soft formation and then drastically to a hard formation due to the content and properties of the formation.

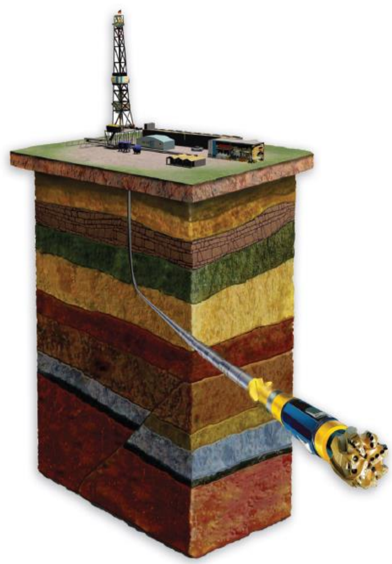

FIGURE 2.2: Multi layer formation

Drilling operation in multi layer formation often takes many trip of drilling as the drill bit has worn out and cause the drilling performance to be undesirable (Hareland, Nygaard & Wise, 2009). During the changing of new drill bit, it uses up a lot of time and this increase the cost of the operation. Meanwhile, this might not only occurred once as if the drilling performance becomes undesirable again or is still undesirable, the drill bit is needed to be taken off and on several times until the case is solved. In this case, it is very important for the selection of a suitable drilling bit to optimize in the run length of the drilling bit rather than only focusing on the penetration rate.

TABLE 2.1: Physical Properties of Rocks

Rock	Dry Density (g/cm^3)	Porosity (%)	Schmidt Hardness Index	Cerchar Abrasivitiy Index
Igneous				
Granite	2.53 – 2.62	1.02 – 2.87	54 – 69	4.5 – 5.3
Diorite	2.80 – 3.00	0.10 – 0.50		4.2 – 5.0
Gabbro	2.72 – 3.00	1.00 – 3.57		3.7 – 4.6
Rhyolite	2.40 – 2.60	0.40 – 4.00		
Andesite	2.50 – 2.80	0.20 – 8.00	67	2.7 – 3.8
Basalt	2.21 – 2.77	0.22 – 22.1	61	2.0 – 3.5
Sedimentary				
Conglomerate	2.47 – 2.76			1.5 – 3.8
Sandstone	1.91 – 2.58	1.62 – 26.4	10 – 37	1.5 – 4.2
Shale	2.00 – 2.40	20.0 – 50.0		0.6 – 1.8
Mudstone	1.82 – 2.72		27	
Dolomite	2.20 – 2.70	0.20 – 4.00		
Limestone	2.67 – 2.72	0.27 – 4.10	35 – 51	1.0 – 2.5
Metamorphic				
Gneiss	2.61 – 3.12	0.32 – 1.16	49	3.5 – 5.3
Schist	2.60 – 2.85	10.0 – 30.0	31	2.2 – 4.5
Phyllite	2.18 – 3.30			
Slate	2.71 – 2.78	1.84 – 3.64		2.3 – 4.2
Marble	2.51 – 2.86	0.65 – 0.81		
Quartzite	2.61 – 2.67	0.40 – 0.65		4.3 – 5.9

TABLE 2.1 shows a list of rocks in different type of rock formations. The main 3 types of rock formation here are igneous formation, sedimentary formation and metamorphic formation. Igneous formation is associated with volcanoes and form at plate boundaries. The rock is formed by molten rock or magma. When the molten rock passes through a cooler region, it cooled up and hardened by going through a process known as fractional crystallization. The formation of igneous formation is fast, while the sedimentary formation needs thousand years to form. Sedimentary rock is formed under the sea bed and layer by layer with the remains of living things, mud, sand, and etc. when the sediment becomes so dense, it undergoes a process called lithification and forms the formation. Last is the metamorphic formation, which is formed when igneous and

sedimentary formations under immerse pressure and heat. The immerse pressure and heat cause the rock to crystallize and form gemstones such as onyx, ruby, sapphire and turquoise.

2.3. Bit Design Parameters

Bit design consists of several parameters, which included the bit profile, bit material, the shape of the cutters, the size of the cutter, the number of back-up cutter, the back rake angle, and gauge design.

The bit profiles that are common seen are double-cone design, parabolic design and concave design. These three designs are normally used in the industry of oil and gas. In the other hand, there are different types of bit material as well, steel, matrix and steel matrix (FIGURE 2.3). The steel body bit is relatively easy to manufacture, while the matrix body bit is too hard to be machined. Matrix body bit is more abrasion and erosion resistance. However, where high impact loads are experienced, matrix body bit is more susceptible to blade breakage than steel. With the idea of combining the advantages of both type of bit material, steel body bit covered with a layer of matrix is introduced. However, coatings and hardfacing have limitations. Their thickness has, for example, tended to be limited by the physical properties of the material or the method of deposition. Hardfacing temperatures can cause material damage to PDC and natural diamond materials, and the manual deposition process requires skill and is expensive.

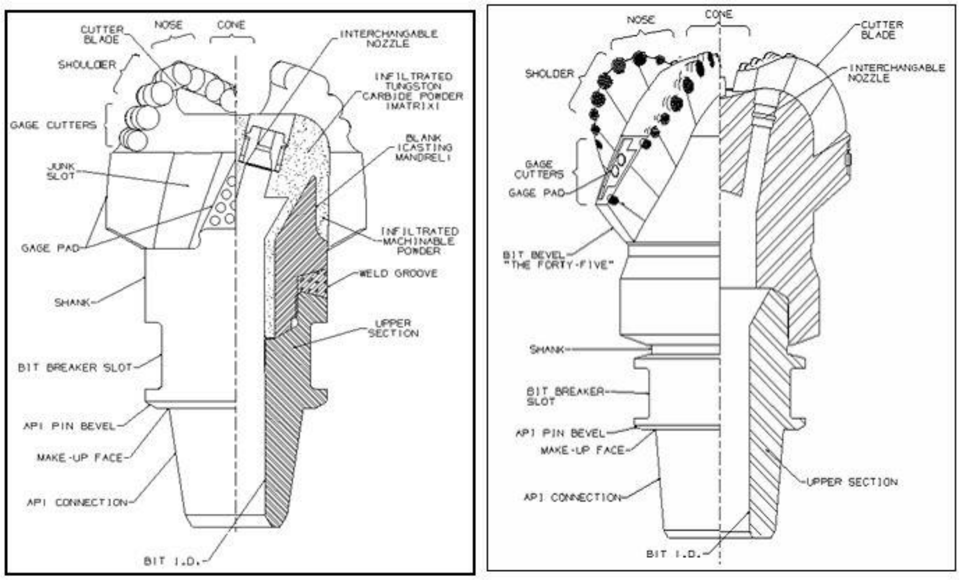

FIGURE 2.3: Matrix body bit (left) & Steel body bit (right)

The shape of the cutter included standard shape, curve shape and cone shape design (FIGURE 2.4). Different shape of the cutter will have a different effect in the removing of cuttings (Motahhari, 2008). When combined together with the other features, it is good to study what shape of cutter will contribute most to the wear rate of the bit.

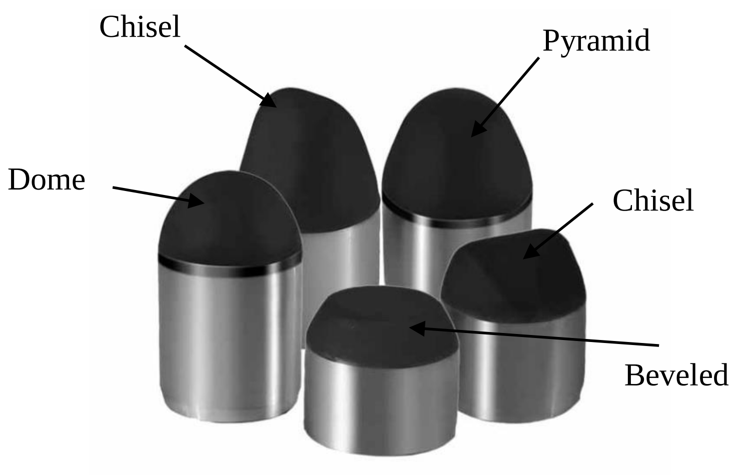

FIGURE 2.4: Sample of different shape of cutters

Generally larger cuttings are produced when using larger cutters (FGURE 2.5). Thus, improving the cleaning in soft formations. It is also believed that certain formations respond more favorably to width of cut than depth of cut. For these, larger cutters that cover a wider lateral area at the expense of reduced penetration will be efficient. Smaller cutters provide long bit life in medium-soft to medium hardness formations. Mid-range cutters respond to a midpoint between the softest and hardest PDC drillable formations.

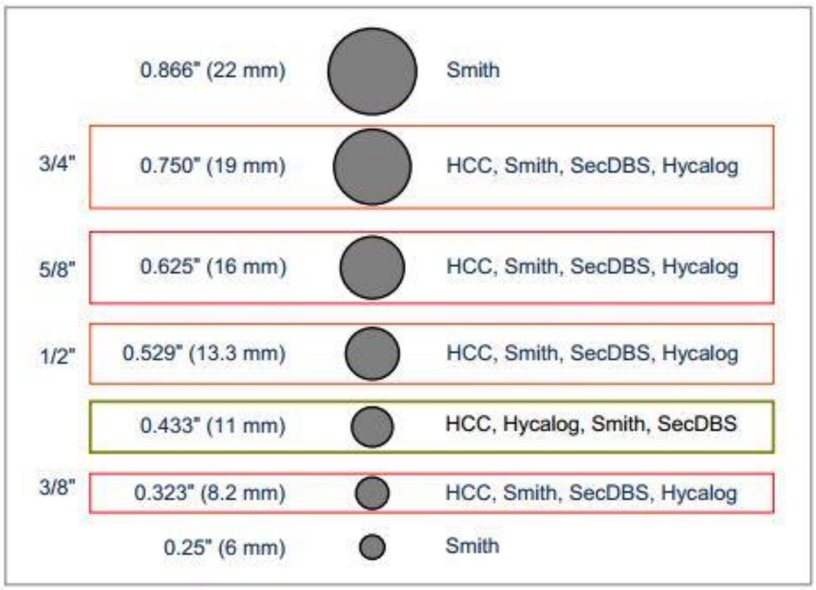

FIGURE 2.5: Series of cutter size

When the bit is used, the first that will wear out are the cutters. Therefore, back-up cutter (FIGURE 2.6) is introduced to increase both the stability and the durability of the bit. When the first roll of cutter is worn out, the back-up cutter still can carry out the drilling process. However, different number of back-up cutter is to be tested for the best drilling performance.

FIGURE 2.6: Back-up cutter

Back rake angle is the specified angle that the PDC bit is set towards to attack the rock of the formation. The lower the back rake angle the more aggressiveness it is of the cutter (Clayton, Chen & Lefort, 2005). Therefore, with the increase the back rake angle indirectly increase the life span of the drill bit. The parameters are set to 0, 5 and 20 degree angle is because the research want to test all type of angle that suit soft shale, abrasive or sandy formation and also the effect of different combinations. Thus different type of angle used in comparison will provide a better comparison effect.

Straight, spiral and spiral track design is introduced to the gauge design. Different type of the gauge design will result in the difference in the stability during the drilling operation (Warrwn & Armegost, 1988).

2.4. Cutter-rock Interaction Modeling

Using the 3D analytical model proposed by Rajabov, et al. (2012), the horizontal cutting force of the PDC cutter can be known by providing the information on the back rake angle and the coefficient of the rock formation.

The forces included in the equation are as following:

- Cutting Force – F_c, acting perpendicular to the cutter surface
- Friction Force, F_{fc}
- Wear Force, F_w, acting perpendicular to the cutter wear flat at the bottom
- Wear Frictional Force, F_{fw}

These forces above are the result of the shearing and friction between the PDC cutter and the crushed rock. Therefore, by balancing the external force on the cutter, the equation below is obtained.

$$F_H = F_C \cos\alpha \cos\beta - F_{fc} \sin\alpha \cos\beta + F_{fw}$$
$$F_S = F_C \cos\alpha \sin\beta - F_{fc} \sin\alpha \sin\beta$$
$$F_N = F_C \sin\alpha - F_{fc} \cos\alpha + F_w$$

Where F_H is the horizontal force, F_S is the shearing force, F_N is the normal force, α is the back rake angle and β is the side rake angle, and

$$F_c = R_c A_c, \quad F_{fc} = \mu F_c = \mu R_c A_c$$
$$F_w = R_p A_w, \qquad F_{fw} = \mu F_w = \mu R_p A_w$$

R_c and R_p are the rock resistance to shearing and rock compressive strength in pounds per square inch (psi) respectively while A_c and A_w are the contact area between cutter and rock, and cutter wear area.

Substituting the values of F_{fc} and F_{fw} from equation to equation, the equation can be yielded respectively:

$$F_c - \mu F_c \tan\alpha = \frac{F_H - \mu F_W}{\cos\alpha\cos\beta}$$

$$F_c - \mu F_c \tan\alpha = \frac{F_S}{\cos\alpha\sin\beta}$$

$$F_c + \mu F_c \cot\alpha = \frac{F_N - F_W}{\sin\alpha}$$

From equation, μF_c can be obtained

$$\mu F_c = \frac{F_N - F_W}{\cos\alpha} - F_c \tan\alpha$$

By substituting and rearranging the equation, following is obtained:

$$F_c = \frac{F_H + F_N \tan\alpha\cos\beta - F_W(\mu + \tan\alpha\cos\beta)}{\cos\alpha\cos\beta\,(1 + \tan^2\alpha)}$$

The equation is then further simplified by assuming the cutter is new, thus the wear force is negligible.

$$F_c = \frac{F_H + F_N \tan\alpha\cos\beta}{\cos\alpha\cos\beta\,(1 + \tan^2\alpha)}$$

With the coefficient of friction known, the equation can be derived into the form:

$$F_c = \frac{F_N}{\sin\alpha - \mu\cos\alpha}$$

And if there is no wear at the cutter, and substitute F_c from equation, the following is obtained:

$$F_H = F_N \cos\beta \left[\frac{1 - \mu\tan\alpha}{\mu + \tan\alpha}\right]$$

Equation shown above is the 3D analytical model that predicts the horizontal cutting force if the normal force and coefficient of friction is known by considering the effect of back rake and side rake angles. If the side rake angle ($\beta = 0$), the equation is simplified to 2D form:

$$F_H = F_N \left[\frac{1 - \mu\tan\alpha}{\mu + \tan\alpha}\right]$$

2.5. Merchant's Model of Orthogonal Cutting

Merchant's model is the first proposed by Dr Merchant to study the forces acting on a tool during the process of metal cutting. By making an analysis of the process on a qualitative basis, the Merchant's model is formed to ease the study of the metal cutting process and the forces relationship.

Several assumptions have been made when Dr Merchant found out the relationship for the forces (Jain & Chitale, 2010):

- The cutting edge of the tool is sharp and it does not make any flank contact with the workpiece.
- Only continuous chip without any built-up edge is produced.
- The shear surface is a plane extending upward from the cutting edge.
- The cutting edge is a straight line, extending perpendicular to the direction of motion, and generates a plane surface as the work moves past it.
- The chip does not flow to either side.

- The cutting velocity remains constant.
- The depth of cut is constant.
- The width of the tool is greater than that of the workpiece.
- The inertia force of the chip is entirely neglected.
- The workpiece moves relative to the tool with uniform velocity.
- The chip behaves as a free body in stable equilibrium under the action of two equal, opposite and almost collinear resultant forces.

The Merchant's circle diagram is shown in Figure 2.7. The terminologies for the diagram are listed below.

- Friction Force – F
- Thrust Force – Ft
- Cutting Force – Fc
- Shear Force – Fs
- Normal Shear Force – Fn
- Normal Frictional Force – N
- Feed Velocity – V
- Rake Angle – α
- Shear Angle – ϕ
- Frictional Angle – β
- Resultant Force - R

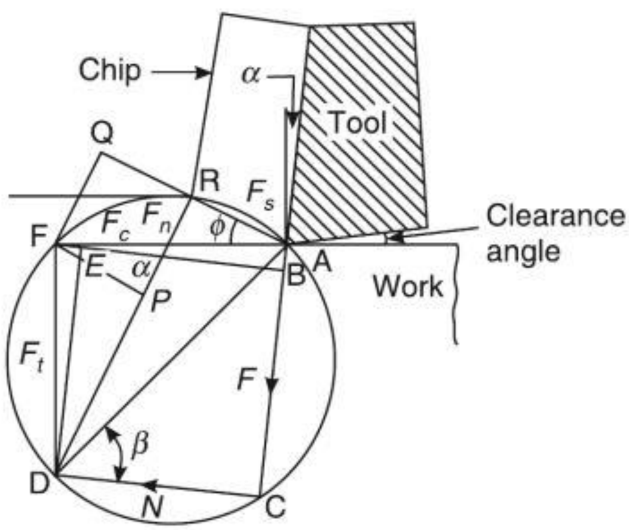

FIGURE 2.7: Merchant's circle diagram

By knowing the Fc, Fs, α, and ϕ, all other component forces can be calculated as:

$$F = F_C \sin\alpha + F_t \cos\alpha$$

$$N = F_C \cos\alpha - F_t \sin\alpha$$

The coefficient of friction will be then given as:

$$\mu = \frac{F}{N} = \frac{F_C \sin\alpha + F_t \cos\alpha}{F_C \cos\alpha - F_t \sin\alpha}$$

On shear plane,

$$F_s = F_C \cos\varphi - F_t \sin\varphi$$

$$F_n = F_C \sin\varphi + F_t \cos\varphi$$

Thus, the resultant force is derived as equation

$$R = \sqrt{{F_c}^2 + {F_t}^2} = \sqrt{{F_s}^2 + {F_n}^2} = \sqrt{F^2 + N^2}$$

The stress on the tool rake face can be obtained using the equation:

$$\sigma = \frac{\text{Normal Frictional Force}}{\text{Contact Area}} = \frac{N}{A}$$

$$\tau = \frac{\text{Shear Force}}{\text{Contact Area}} = \frac{F}{A}$$

2.6. Stress Analysis

When a body is subjected to axial force and torsional force, axial stress and torsional stress are produced.

Based on Hibbeler (2013), the axial stress, σ is obtained using equation :

$$\sigma = \frac{F}{A}$$

where F and A is the axial force and A is the loading area. The axial strain, ε can be obtained using equation:

$$\varepsilon = \frac{\sigma}{E}$$

where E is the Young's Modulus of the material of the body.

Torsion acting on a cylinder tends to twist it in the direction of the torque. The assumptions are made for the body:

- Plane sections remain plane after the torque is applied
- The shear strain γ varies linearly in the radial direction
- The material is linearly elastic, so that Hooke's law applies

The maximum shear stress (τ_{max}) occurs in a circular body of radius due to the application of torque is calculated using equation:

$$\tau_{max} = \frac{Tr}{J}$$

Where T is the torque, r is the radius of the body and J is the polar moment of inertia of the cross sectional area.

The polar moment of inertia of the cross sectional area is:

$$J = \frac{\pi}{2r^4}$$

According to the maximum distortion energy criterion, the failure occurs when the maximum shear stress (τ_{yield}) reaches $\frac{\sqrt{2}\sigma_y}{3}$ if the maximum shear stress theory is valid. And the angle of twist, φ can be found by using:

$$\varphi = \frac{TL}{GJ}$$

where L is the length of the body and G is the shear modulus of the body material. This value is dependent on the material properties.

2.7. Wear Model

A wear model which indicates that the total tribological system determines the wear behavior is proposed while von mises stress is related to wear by calculating the wear volume per unit distance, W in μm^2 using equation (Tangena, 1990):

$$W = k_2 V \bar{\sigma}^{\frac{1}{bn'}}$$

where k_2 is an arbitrary wear constant, V is the deformed volume, $\bar{\sigma}$ is the von Mises stress in MPa, b is a constant whose value is approximately 0.5, and n' is the cyclic strain-hardening coefficient which is equal to 0.31. Value of $\frac{1}{bn'}$ is around 6.45, typically. The large value of this coefficient points out that the von Mises stress in the stressed volume is dominant in the wear process and will significantly response to the wear value. The contact geometry, the mechanical properties of the materials, the friction and the externally applied forces vary the magnitude of the von Mises stress. The proportionality constant $k_2 \times V$ was taken as 1.5 x 10^{-11}. For the system, the deformed volume, V is equal to$\pi a^2 d$, where a is the contact radius and d is the thickness of layer. Table 2.2 below shows the list of coefficient with different type of material.

TABLE 2.2 Ludwik Relationship of Different Materials

(Tangena, 1988 and Schouwenaars et al., 2009)

Material	**Constant, K (N/mm^2)**	**Strain-hardening coefficient, n′**	**Power, $\frac{1}{bn'}$**	**Proportionality Constant, k_2V**
Gold (Au)	478	0.63	3.15	3.36 x 10^{-2}
Polycrystalline Diamond (PCD)	573	0.31	6.45	1.50 x 10^{-11}
Nickel (Ni)	4889	0.55	3.64	3.45 x 10^{-7}
Copper (Cu)	530	0.44	4.55	3.72 x 10^{-6}
304 Stainless Steel	1400	0.44	4.55	4.48 x 10^{-6}

Chapter 3

Methodology

3.1. Framework

PARAMETERS:

1. The parameters which chosen for the project is:

   (i) Size of the Cutter & (ii) Shape of the Cutter.

2. Other parameters of the cutter are remained constant and the assumed to be working perfectly.

↓

ANALYTICAL MODEL:

1. An analytical model is derived to compute the functional forces of a PDC bit during a drilling operation.
2. The functional forces are:
   a. Axial Stress
   b. Shear Stress

↓

ABAQUS (Part 1):

1. A 3D CAD model is prepared using CATIA software and saved as igs file which later be used in ABAQUS.
2. The properties of the PDC bit and the formation is input into the system after importing the 3D CAD model.

↓

ABAQUS (Part 2):

3. The parts are paired with the respective properties and meshed.
   a. Johnson-Cook Damage (Damage Evolution)
   b. Density
   c. Elastic
   d. Plastic
4. The step of the simulation is set.
   a. Dynamic, Explicit, Energy
5. Interaction Properties is chosen and set.
   a. General Contact, Tangential Behavior, Penalty
6. Constraints are set at the contact surface.
7. Amplitude is defined as tabular for the simulation.
8. Body conditions defined for the Bit and Formation.
   a. Formation, Displacement (Static)
   b. Bit, Velocity/Angular Velocity
9. Job is created for the model and data submitted for simulation.

↓

RESULTS:

1. The result obtained from ABAQUS is validated and verified.
2. Establish the relationship between stress and wear.
3. Tabulate and analysis the data.
4. Generate and determine the effect of size and shape of cutter.

FIGURE 3.1: Research Methodology

3.2. Reverse Engineering

Reverse engineering is used in the project to get the 3D Computer-Aided-Design (CAD) model of the conventional PDC bit which is provided by the Petroleum Department of Universiti Teknologi PETRONAS (UTP). The TABLE 3.1 shows the specifications of the PDC bit used.

TABLE 3.1: Product Specifications

Nomenclature	M50BPX
Size	6 in
No. of Blades	6
Cutter Quantity	34
No. of Nozzles	3
Connection	3 ½ API REG
Manufacturer	SMITH

3.3. 3D scanning

The VIUscan Scanner (FIGURE 3.2) scan the dull PDC drill bit obtained from UTP and the details are transferred to the Cloud Model display. The noise and the facets of the model are removed using the software called VXelement. Then the 3D CAD model is generated using the GeoMagic 12 to redesign.

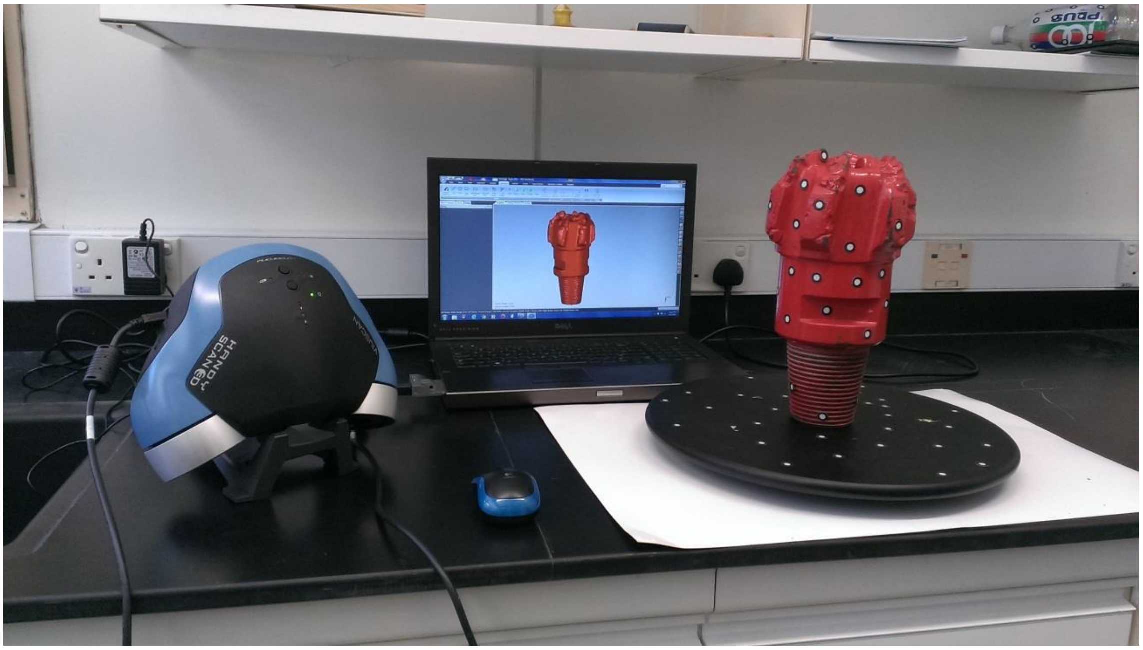

FIGURE 3.2: VIUscan Scanner, Clould Model display and dull PDC drill bit (left to right)

3.4. Parameters

TABLE 3.2 shows the constant parameters in the project.

TABLE 3.2: Parameters of PDC bit

Bit Body	
Bit Size	215.9 mm (8.5 in.)
Bit Body Material	Tungsten Carbide Matrix
Bit Profile	Concave
Polycrystalline Diamond Compact (PDC) Cutter	
Size of Cutter	**6mm – 22mm**
Type of Cutter	Polycrystalline Diamond (PCD) bonded with tungsten carbide-cobalt (WC-Co)
Shape of Cutter	**Cylindrical (Standard, Cone, Curve)**
Backup cutters	-
Cutter Edge Chamfer	45 °(curve cutter only)
Cutter Edge Geometry	0.254 mm (0.010 in.) (curve cutter only)
Diamond Carbide Interface	Conventional
Back Rake Angle	15 °
Blade	
Number of Blades	6
Junk Slot	
Junk Slot Area	Fixed
Face Volume	Fixed
Gauge	
Gauge Design	Spiral
Gauge Length	63.55 mm (2.5 in.)
Gauge Cutters	-

TABLE 3.3 shows the operating variables in the project.

TABLE 3.3: Operating Variables

Parameter	Value
Weight on Bit (WOB)	25k lb
Rotation per minute (RPM)	170 rpm

TABLE 3.4 shows the mechanical properties of the bit body.

TABLE 3.4: Mechanical Properties of bit body

	Steel	Matrix(Tungsten Carbide)
Density ($kg \cdot m^{-3}$)	**3510**	**15880**
Thermal Conductivity ($W \cdot m^{-1} \cdot K^{-1}$)	**543**	**88**
Specific Heat ($J \cdot kg^{-1} \cdot K^{-1}$)	**790**	**184**
Thermal Expansion Coefficient ($10^{-6} K^{-1}$)	**2.5**	**7.1**
Young's Modulus (GPa)	**890**	**686**
Poisson Ratio	**0.07**	**0.22**
Shear Modulus (GPa)	**79.3**	**283**

TABLE 3.5 shows the mechanical properties of the PDC cutter.

TABLE 3.5: Mechanical Properties of PDC cutter (Yahiaoui et al., 2012)

	PCD	WC-Co
Density ($\boldsymbol{kg \cdot m^{-3}}$)	**3510**	**15000**
Thermal Conductivity ($\boldsymbol{W \cdot m^{-1} \cdot K^{-1}}$)	**543**	**100**
Specific Heat ($\boldsymbol{J \cdot kg^{-1} \cdot K^{-1}}$)	**790**	**230**
Thermal Expansion Coefficient ($\boldsymbol{10^{-6} K^{-1}}$)	**2.5**	**5.2**
Young's Modulus ($\boldsymbol{GPa}$)	**890**	**579**
Shear Modulus ($\boldsymbol{GPa}$)	**545**	**280**
Poisson Ratio	**0.07**	**0.22**

TABLE 3.6 shows the properties for the formation:

TABLE 3.6: Properties of Formations

	Sandstone	**Dolomite**
Density ($\boldsymbol{kg \cdot m^{-3}}$)	**1910**	**2700**
UC Strength ($\boldsymbol{MPa}$)	**50**	**170**
Thermal Conductivity ($\boldsymbol{W \cdot m^{-1} \cdot K^{-1}}$)	**2.5**	**5.1**
Specific Heat ($\boldsymbol{J \cdot kg^{-1} \cdot K^{-1}}$)	**920**	**920**
Thermal Expansion Coefficient ($\boldsymbol{10^{-6} K^{-1}}$)	**11.6**	**10.0**
Elastic Modulus ($\boldsymbol{GPa}$)	**15**	**70**
Yield Strength ($\boldsymbol{MPa}$)	**4**	**15**
Poisson Ratio	**0.14**	**0.15**
Coefficient of Friction	**0.51**	**1.00**

3.5. Design Features

FIGURE 3.3 is the bit design features selected for the project. The following included the size of cutters and the shape of the cutters.

Size of Cutters	8 mm	13 mm	16 mm
Isometric	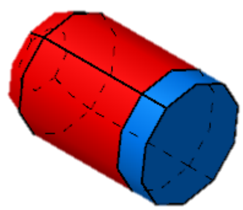	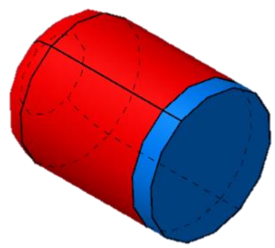	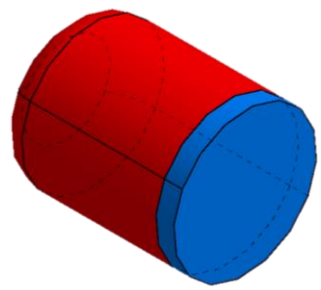
	a(i)	**a(ii)**	**a(iii)**

Shape of Cutters	Standard	Curve	Cone
Isometric	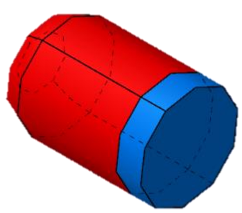	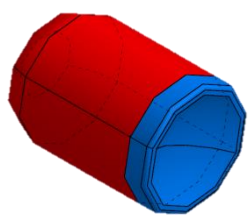	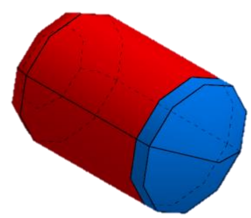
	b(i)	**b(ii)**	**b(iii)**

FIGURE 3.3: a(i) 8mm bit cutter. a(ii) 13mm bit cutter. a(iii) 16mm bit cutter. b(i) standard shape cutter. b(ii) curve shape cutter. b(iii) cone shape cutter.

3.6. Gantt Chart

TABLE 3.7: Gantt Chart and Key Milestone (FYP 1)

No	Activities/Week	1	2	3	4	5	6	7	8	9	10	11	12	13	14
1	Literature Review related to drill bit and drilling operation														
2	Preliminary Research Work on how to simulate bit wear using existing software														
3	Software Learning														
4	Bit Design Parameters Determination														
5	Drill Bit Model Selection														
6	KSB Trip														
7	Research on data and findings of Multi-layer Formation														
8	Bit Wear Rate Simulation on Multi-layer Formation														

	Process
	Key Milestone

TABLE 3.8: Gantt Chart and Key Milestone (FYP 2)

No	Activities/Week	1	2	3	4	5	6	7	8	9	10	11	12	13	14
1	Bit Wear Rate Simulation on Multi-layer Formation	█	█	█	█	█									
2	Completed Simulation					●									
3	Analysis on the result					█	█	█	█						
4	Conclusion and Recommendation								█	●					
5	Best Bit Design Sellection									●					
6	Pre-SEDEX										●				
7	SEDEX											●			

█	Process
●	Key Milestone

Chapter 4

Result & Discussion

4.1. PDC SINGLE CUTTER TEST

PART I: PDC SINGLE CUTTER ANALYTICAL MODEL

4.1.1. Size of the cutter

Table 4.1 shows the single cutter data for different sizes.

TABLE 4.1: Single Cutter Data (Size of Cutter)

Size of Cutter	8mm	13mm	16mm
Shape the Cutter	Flat	Flat	Flat
Normal Force, F_N	1400 N	2300 N	2500 N
Shear Contact Area, A_S	2.51E-05	6.64E-05	1.01E-04

Half of the cutting face surface area is taken into calculation for the shear stress as the depth of cut is half of the cutter diameter.

Below is the equation used for the computation of horizontal force:

$$F_H = F_N \left[\frac{1 - \mu \tan \alpha}{\tan \alpha + \mu} \right]$$

Table 4.2 shows the horizontal force for different size of cutter.

TABLE 4.2: Horizontal Force for Different Size of Cutter

Size of Cutter	**Horizontal Force, F_H (N)**	
	Sandstone Formation	**Dolomite Formation**
8mm	1553.68	808.29
13mm	2552.48	1327.91
16mm	2774.43	1443.38

The result shows that the cutter with a smaller size has relatively smaller horizontal force when compared to the other 2 sizes. As the back rake angle is the same for all cutters, the only variable in the equation is the applied normal force, which is subjected to the size of the cutter. The difference in the normal force is due to the difference in number of cutter on the bit due to the difference in size.

Referring to Merchant's model, the equation below is used to calculate the shear stress on the cutter face:

$$\tau = \frac{\text{Horizontal Force}}{\text{Shear Contact Area}} = \frac{F_H}{A_S}$$

Table 4.3 shows the result of the shear stress for different size of cutter.

TABLE 4.3: Calculated Shear Stress for Different Size of Cutter

Size of Cutter	**Shear Stress, τ (MPa)**	
	Sandstone Formation	**Dolomite Formation**
8mm	6.18E+01	3.22E+01
13mm	3.85E+01	2.00E+01
16mm	2.76E+01	1.44E+01

Figure 4.1 shows the chart of shear stress against the size of cutter on sandstone and dolomite formation.

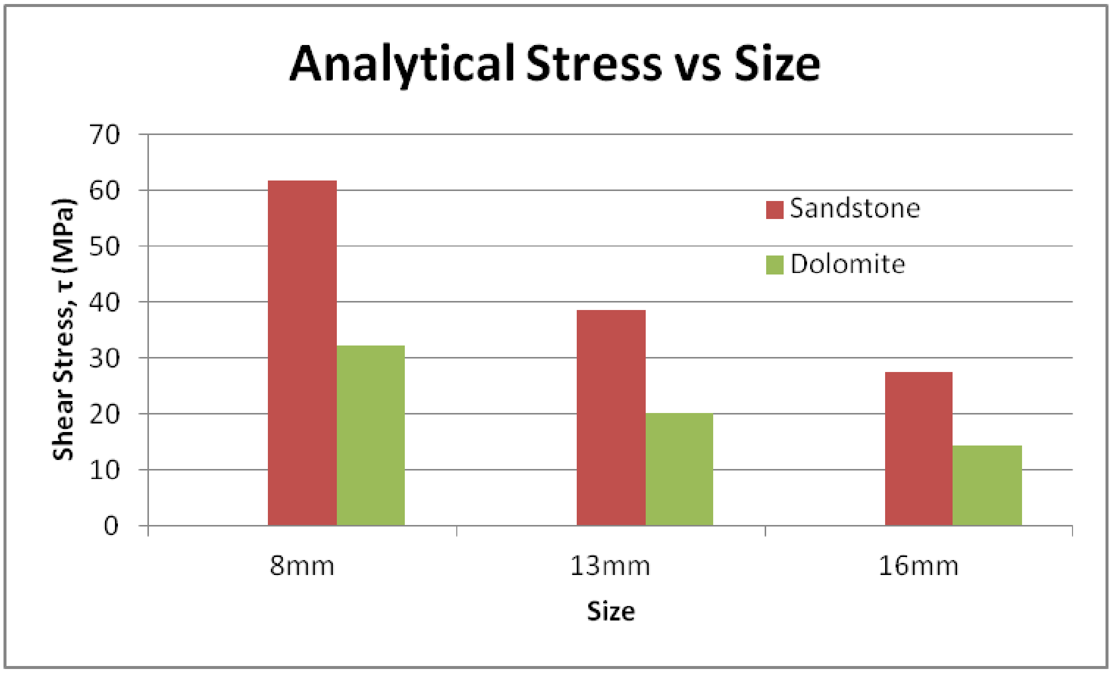

FIGURE 4.1: Effect on Size of Cutter on Shear Stress (Analytical)

The result shows that the cutter with the size of 16mm experiences less shear stress. This is because of the decreased in the size of the cutter, which is the shear contact area of the cutter. By lowering the stress exerted on the cutter face, the cutter durability improves. Therefore, PDC cutter with the size of 16mm recommended for the formation drilling application based on the analytical model made using excel.

4.1.2. Shape of Cutter

Three different type of cutter are used for the analytical model, which is flat, curved and cone, while the other factors such as the back rake angle remained constant. Since the cutter back rake angle is constant, the applied horizontal force is constant for all shapes of cutter as there are no changes on the applied normal force. Half of the cutting face surface area is taken into calculation for the shear stress as the depth of cut is half of the cutter diameter.

Table 4.4 shows the single cutter data for different shapes.

TABLE 4.4: Single Cutter Data (Shape of Cutter)

Size of Cutter	16mm	16mm	16mm
Shape of Cutter	Flat	Curved	Cone
Normal Force, F_N	2500 N	2500 N	2500 N
Shear Contact Area, A_S	1.01E-04	1.09E-04	1.40E-04

Table 4.5 shows the result of the horizontal force for different shape of cutter.

TABLE 4.5: Horizontal Force for Different Size of Cutter

Shape of Cutter	**Horizontal Force, F_H (N)**	
	Sandstone Formation	**Dolomite Formation**
Flat	2774.43	1443.38
Curved	2774.43	1443.38
Cone	2774.43	1443.38

The table shows constant horizontal force for all three type of shape of the cutter as the shape of cutter result in the change in shear contact area only. With the applied normal force and back rake angle as constant, there are no changes in the horizontal force.

Then, the shear contact area for different shapes of cutter is used to calculate the shear stress using same equation as the previous:

$$\tau = \frac{\text{Horizontal Force}}{\text{Shear Contact Area}} = \frac{F_H}{A_S}$$

Table 4.6 shows the result of the shear stress for different shape of cutter.

TABLE 4.6: Calculated Shear Stress for Different Shape of Cutter

Shape of Cutter	**Shear Stress, τ (MPa)**	
	Sandstone Formation	**Dolomite Formation**
Flat	2.76E+01	1.44E+01
Curved	2.54E+01	1.32E+01
Cone	1.99E+01	1.03E+01

Figure 4.2 shows the chart of shear stress against the shape of cutter on sandstone and dolomite formation.

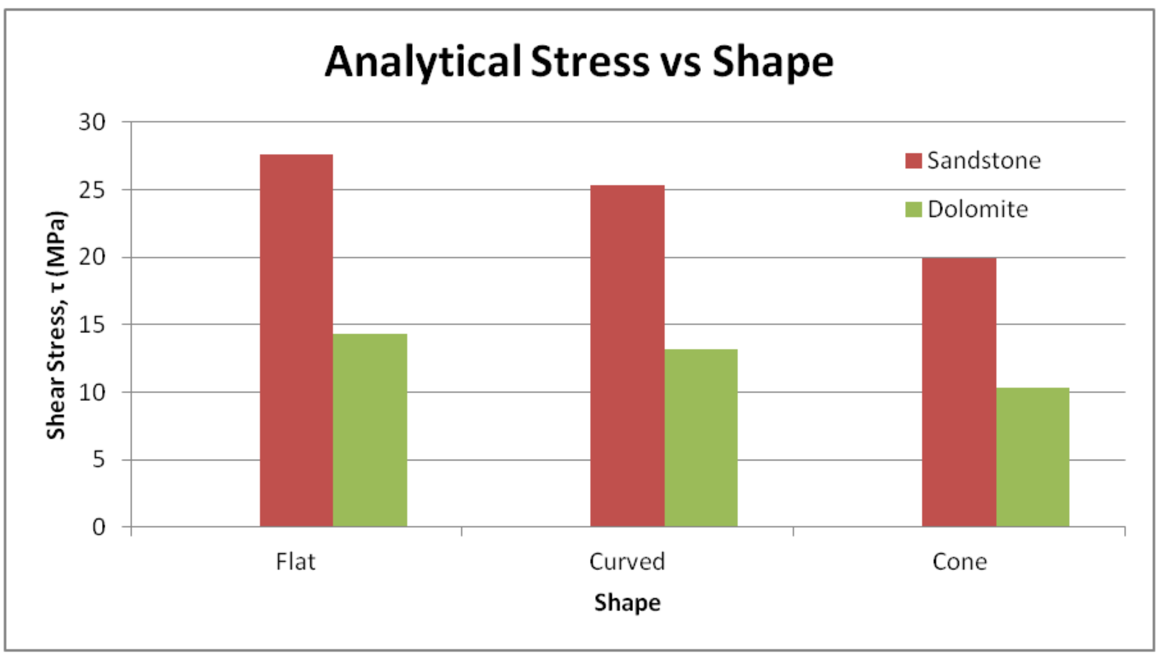

FIGURE 4.2: Effect on Shape of Cutter on Shear Stress (Analytical)

Based on the result shows in Figure 27, cone shape cutter has the least shear stress compared to the other 2 type of shape. The reduced in shear stress is due to the increase in shear contact area of the cone shape cutter. Therefore, to increase the cutter durability, cone size cutter with a relatively larger shear contact area is preferable.

PART II: PDC SINGLE CUTTER SIMULATION

4.1.3. Size of Cutter

Table 4.7 shows the simulation data of von Mises stress for different size of cutter for sandstone formation.

TABLE 4.7: Simulation Data for Different Size of Cutter (Sandstone Formation)

	Size of Cutter		
	8mm	13mm	16mm
Time (s)	**Stress (Pa) – Sandstone Formation**		
0.0	0	0	0
2.5	5.02E+06	1.65E+06	2.36E+06
5.0	1.49E+07	5.92E+06	5.32E+06
7.5	2.58E+07	9.86E+06	7.26E+06
10.0	3.65E+07	1.43E+07	1.12E+07
12.5	4.59E+07	1.89E+07	1.61E+07
15.0	5.63E+07	2.30E+07	2.05E+07
17.5	6.60E+07	2.74E+07	2.49E+07
20.0	7.35E+07	3.18E+07	2.85E+07
22.5	8.11E+07	3.63E+07	3.15E+07
25.0	9.00E+07	4.13E+07	3.43E+07
27.5	9.33E+07	4.40E+07	3.42E+07
30.0	9.39E+07	4.28E+07	3.46E+07
32.5	9.43E+07	4.30E+07	3.50E+07
35.0	9.39E+07	4.27E+07	3.48E+07
37.5	9.20E+07	4.30E+07	3.53E+07

40.0	9.29E+07	4.29E+07	3.54E+07
42.5	9.16E+07	4.22E+07	3.52E+07
45.0	9.48E+07	4.37E+07	3.49E+07
47.5	9.04E+07	4.33E+07	3.42E+07
50.0	9.35E+07	4.28E+07	3.54E+07
52.5	9.06E+07	4.38E+07	3.58E+07
55.0	9.45E+07	4.29E+07	3.53E+07
57.5	9.14E+07	4.31E+07	3.58E+07
60.0	9.09E+07	4.30E+07	3.51E+07

Table 4.8 shows the simulation data of von Mises stress for different size of cutter for dolomite formation.

TABLE 4.8: Simulation Data for Different Size of Cutter (Dolomite Formation)

	Size of Cutter		
	8mm	**13mm**	**16mm**
Time (s)	**Stress (Pa) – Dolomite Formation**		
0.0	0	0	0
2.5	2.51E+06	8.23E+05	1.18E+06
5.0	7.44E+06	2.96E+06	2.66E+06
7.5	1.29E+07	4.93E+06	3.63E+06
10.0	1.83E+07	7.15E+06	5.62E+06
12.5	2.29E+07	9.45E+06	8.07E+06
15.0	2.81E+07	1.15E+07	1.03E+07
17.5	3.30E+07	1.37E+07	1.25E+07
20.0	3.67E+07	1.59E+07	1.43E+07

22.5	4.06E+07	1.81E+07	1.57E+07
25.0	4.50E+07	2.06E+07	1.72E+07
27.5	4.67E+07	2.20E+07	1.71E+07
30.0	4.69E+07	2.24E+07	1.73E+07
32.5	4.72E+07	2.15E+07	1.75E+07
35.0	4.69E+07	2.14E+07	1.74E+07
37.5	4.60E+07	2.15E+07	1.76E+07
40.0	4.65E+07	2.15E+07	1.77E+07
42.5	4.68E+07	2.11E+07	1.76E+07
45.0	4.74E+07	2.18E+07	1.74E+07
47.5	4.62E+07	2.16E+07	1.71E+07
50.0	4.68E+07	2.19E+07	1.77E+07
52.5	4.68E+07	2.19E+07	1.79E+07
55.0	4.63E+07	2.19E+07	1.76E+07
57.5	4.67E+07	2.16E+07	1.79E+07
60.0	4.55E+07	2.15E+07	1.76E+07

Figure 4.3 and Figure 4.4 below show the graph of stress against time for different size of cutter for sandstone and dolomite formations plotted with the simulation data shown above.

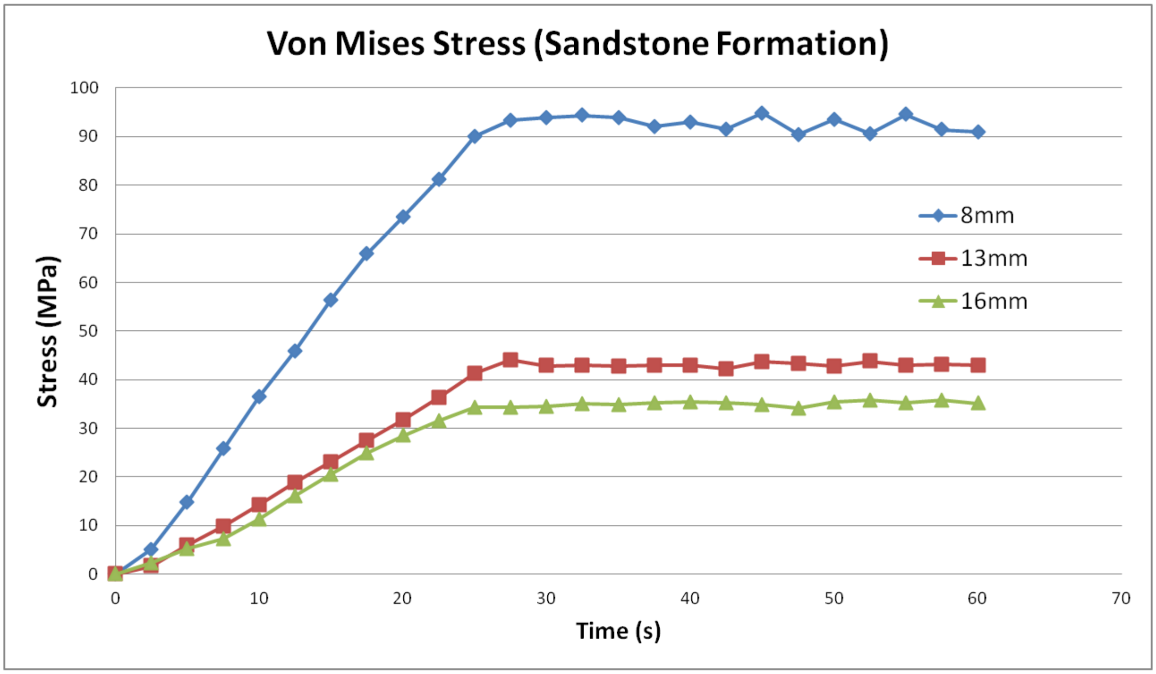

FIGURE 4.3: Graph of Stress vs Time for Different Size of Cutter (Sandstone Formation)

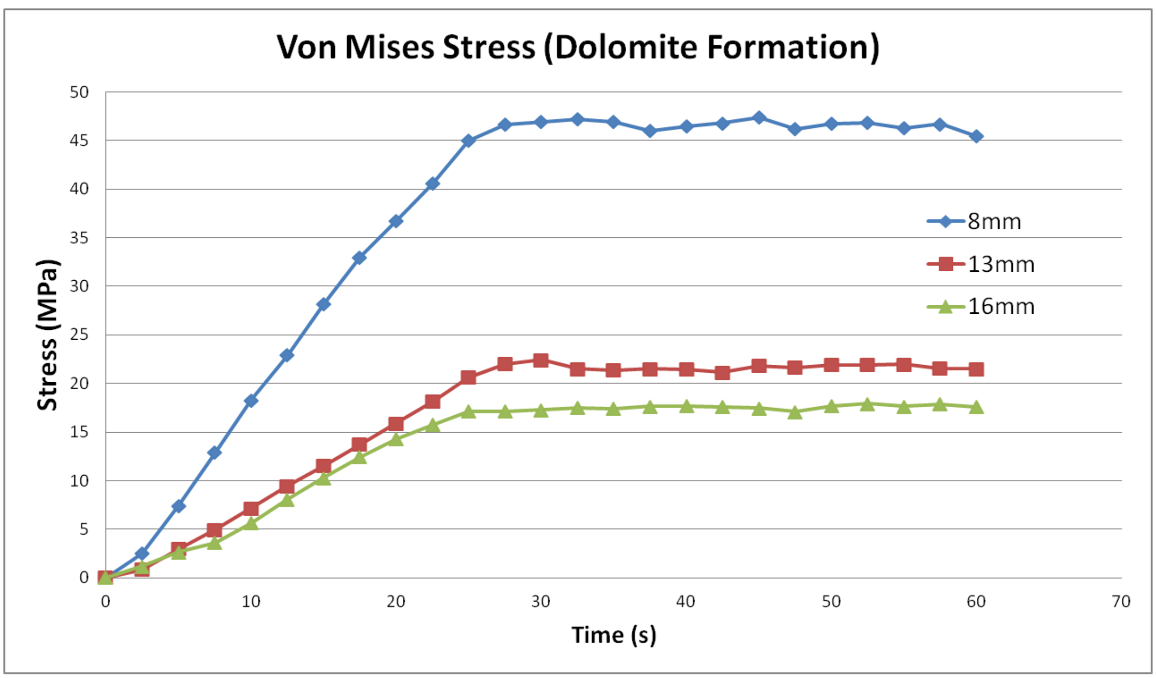

FIGURE 4.4: Graph of Stress vs Time for Different Size of Cutter (Dolomite Formation)

The stress of the cutter climb rapidly in the beginning and started to stable itself about 30s afterwards. This is because the simulated data is trying to reach the designated horizontal force during the beginning stage of the simulation.

The average stress after it stabilizes is taken for comparison with the analytical data. The average von Mises stress induced in PDC cutter with different size of cutter for both formations is tabulated in Table 4.9 below respectively.

TABLE 4.9: Average Stress for Different Size of Cutter

Size of Cutter	Average Stress (MPa)	
	Sandstone Formation	Dolomite Formation
8mm	9.25E+07	4.65E+07
13mm	4.30E+07	2.16E+07
16mm	3.50E+07	1.75E+07

Figure 4.5 shows the chart of simulated shear stress against the size of cutter on sandstone and dolomite formation.

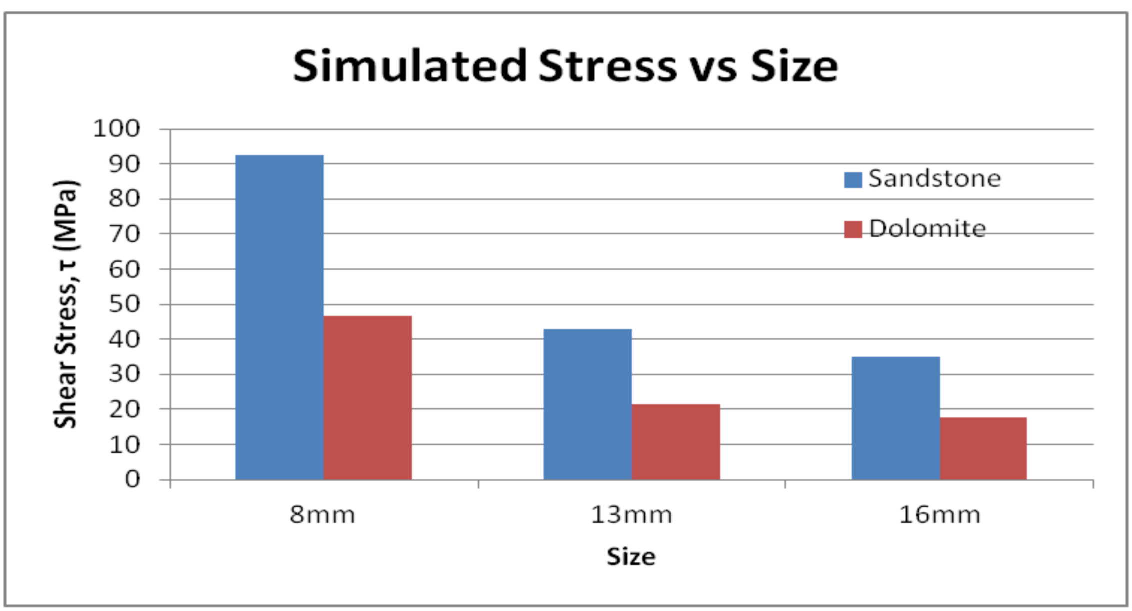

FIGURE 4.5: Effect on Size of Cutter on Shear Stress (Simulation)

From the simulated result, the cutter with size of 16mm is best for the drilling application as it has the lowest stress compared to the other 2 sizes. This result is good, as it tally with the equation findings with the analytical data and shows a same relationship.

Table 4.10 shows the comparison between the simulation data and the analytical data.

TABLE 4.10: Stress Values for Different Size of Cutter

	Sandstone Formation		**Dolomite Formation**	
Size of Cutter	**Simulated Stress (MPa)**	**Analytical Stress (MPa)**	**Simulated Stress (MPa)**	**Analytical Stress (MPa)**
8mm	9.25E+07	6.18E+01	4.65E+07	3.22E+01
13mm	4.30E+07	3.85E+01	2.16E+07	2.00E+01
16mm	3.50E+07	2.76E+01	1.75E+07	1.44E+01

Figure 4.6 shows the comparison between simulated stress and analytical stress for different size of cutter.

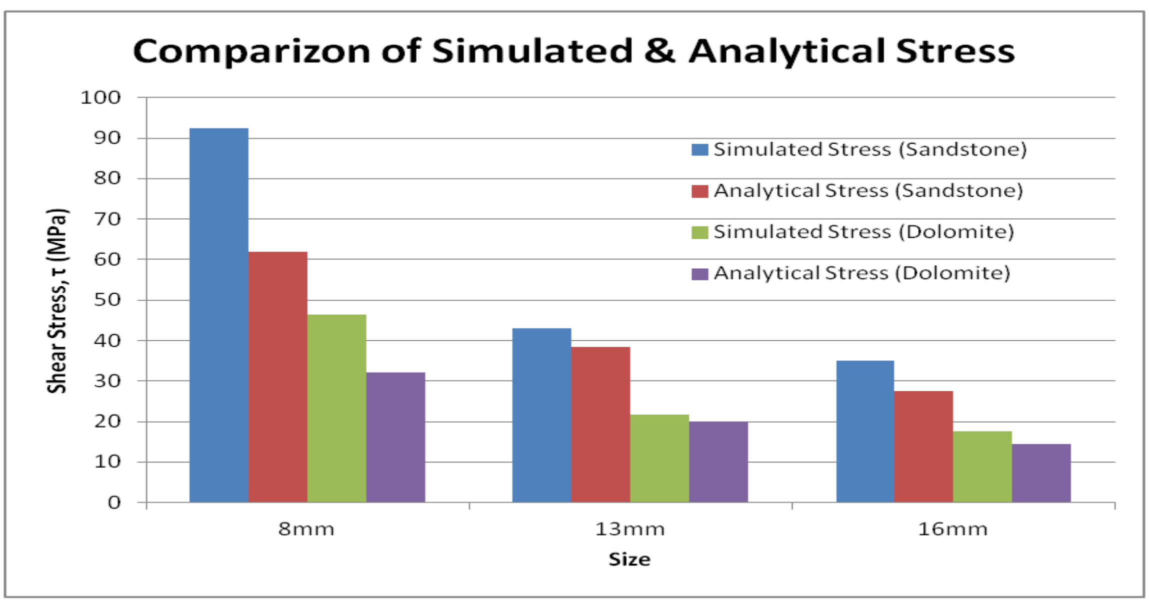

FIGURE 4.6: Comparison of Stress Values for Different Size of Cutter

The von Mises stress obtained from the simulation data is higher than analytical data. This is due to the axial stress and not all forces are taken into the calculation of the analytical model. However, both the simulated and analytical stress data show the same behaviour, which tally with the theory based on the equation. Thus, both set of data show that the best size of cutter for drilling operation in considerations of cutter durability is the cutter with 16mm size.

4.1.4. Shape of Cutter

Table 4.11 shows the simulation data of von Mises stress for different shape of cutter for sandstone formation.

TABLE 4.11: Simulation Data for Different Shape of Cutter (Sandstone Formation)

	Shape of Cutter		
	Flat	Curved	Cone
Time (s)	Stress (Pa) – Sandstone Formation		
0.0	0	0	0
2.5	2.36.E+06	2.86E+06	3.39E+06
5.0	5.32.E+06	6.07E+06	5.42E+06
7.5	7.26.E+06	9.80E+06	7.56E+06
10.0	1.12.E+07	1.38E+07	9.45E+06
12.5	1.61.E+07	1.73E+07	1.21E+07
15.0	2.05.E+07	2.11E+07	1.53E+07
17.5	2.49.E+07	2.38E+07	1.62E+07
20.0	2.85.E+07	2.54E+07	1.70E+07
22.5	3.15.E+07	2.53E+07	1.78E+07
25.0	3.43.E+07	2.62E+07	1.87E+07
27.5	3.42.E+07	28369080	2.07E+07

30.0	3.46.E+07	28944900	2.30E+07
32.5	3.50.E+07	28081260	2.38E+07
35.0	3.48.E+07	28421730	2.49E+07
37.5	3.53.E+07	28061730	2.56E+07
40.0	3.54.E+07	27521730	2.47E+07
42.5	3.52.E+07	27341730	2.47E+07
45.0	3.49.E+07	27431730	2.42E+07
47.5	3.42.E+07	28061730	2.47E+07
50.0	3.54.E+07	28241730	2.50E+07
52.5	3.58.E+07	28888173	2.49E+07
55.0	3.53.E+07	28061730	2.43E+07
57.5	3.58.E+07	28331730	2.45E+07
60.0	3.51.E+07	27971730	2.45E+07

Table 4.12 shows the simulation data of von Mises stress for different shape of cutter for dolomite formation.

TABLE 4.12: Simulation Data for Different Shape of Cutter (Dolomite Formation)

	Shape of Cutter		
	Flat	**Curved**	**Cone**
Time (s)	**Stress (Pa) – Dolomite Formation**		
0.0	0	0	0
2.5	1.18E+06	1.37E+06	1.63E+06
5.0	2.66E+06	2.91E+06	2.60E+06
7.5	3.63E+06	4.70E+06	3.63E+06
10.0	5.62E+06	6.62E+06	4.54E+06

12.5	8.07E+06	8.30E+06	5.81E+06
15.0	1.03E+07	1.01E+07	7.33E+06
17.5	1.25E+07	1.14E+07	7.76E+06
20.0	1.43E+07	1.22E+07	8.15E+06
22.5	1.57E+07	1.22E+07	8.52E+06
25.0	1.72E+07	1.26E+07	8.99E+06
27.5	1.71E+07	1.36E+07	9.96E+06
30.0	1.73E+07	1.39E+07	1.10E+07
32.5	1.75E+07	1.35E+07	1.14E+07
35.0	1.74E+07	1.36E+07	1.19E+07
37.5	1.76E+07	1.35E+07	1.20E+07
40.0	1.77E+07	1.32E+07	1.19E+07
42.5	1.76E+07	1.31E+07	1.18E+07
45.0	1.74E+07	1.38E+07	1.16E+07
47.5	1.71E+07	1.35E+07	1.16E+07
50.0	1.77E+07	1.37E+07	1.20E+07
52.5	1.79E+07	1.39E+07	1.20E+07
55.0	1.76E+07	1.35E+07	1.17E+07
57.5	1.79E+07	1.36E+07	1.18E+07
60.0	1.76E+07	1.34E+07	1.18E+07

Figure 4.7 and Figure 4.8 show the graph of stress against time for different size of cutter for sandstone and dolomite formations plotted with the simulation data shown above.

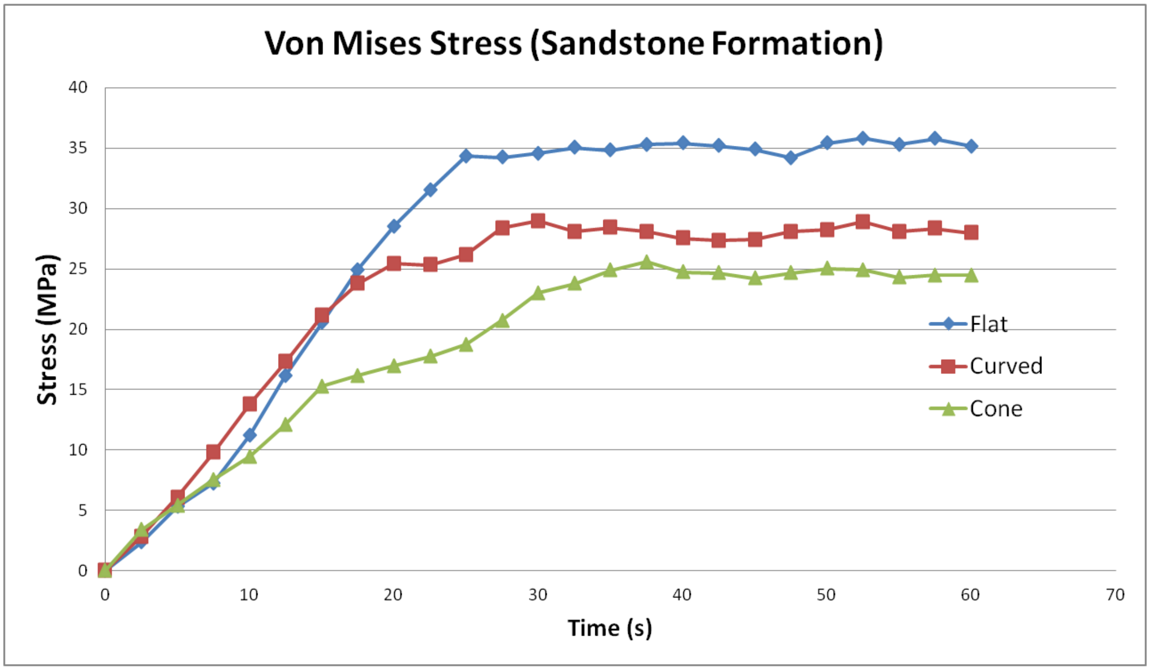

FIGURE 4.7: Graph of Stress vs Time for Different Shape of Cutter (Sandstone Formation)

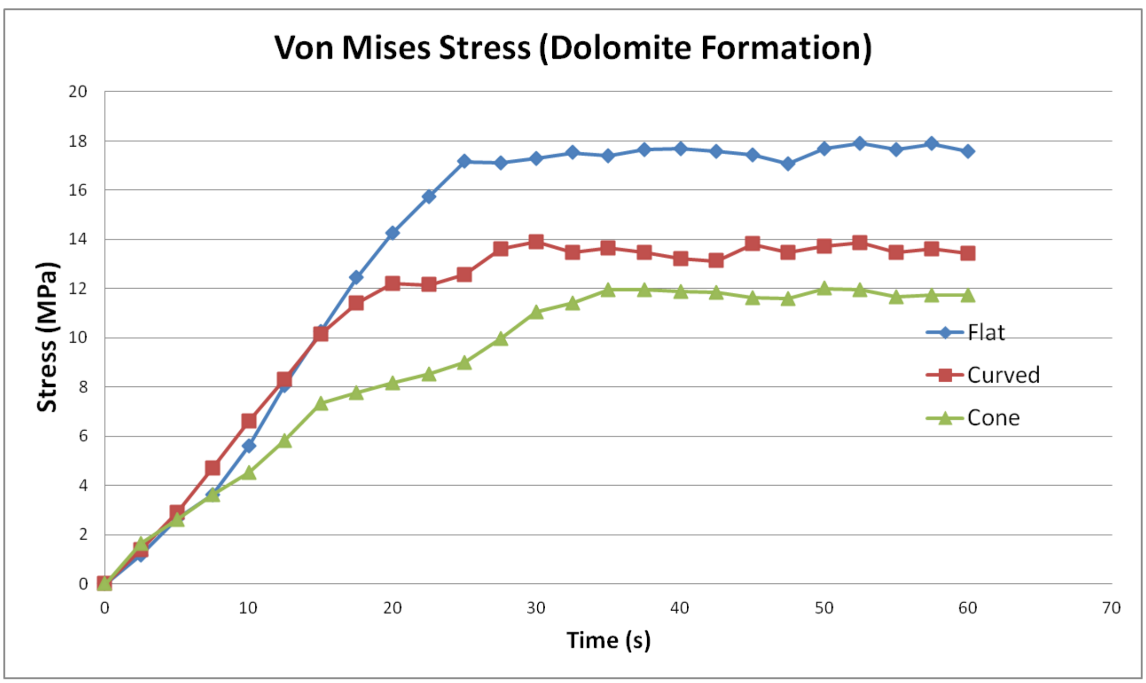

FIGURE 4.8: Graph of Stress vs Time for Different Shape of Cutter (Dolomite Formation)

The average stress after about 30s is taken for comparison with the analytical data. The average von Mises stress induced in PDC cutter with different shape of cutter for both formations is tabulated in Table 4.13 below respectively.

TABLE 4.13: Average Stress for Different Shape of Cutter

Shape of Cutter	**Average Stress (MPa)**	
	Sandstone Formation	**Dolomite Formation**
Flat	3.50E+01	1.75E+01
Curved	2.80E+01	1.35E+01
Cone	2.39E+01	1.14E+01

Figure 4.9 shows the chart of simulated shear stress against the shape of cutter on sandstone and dolomite formation.

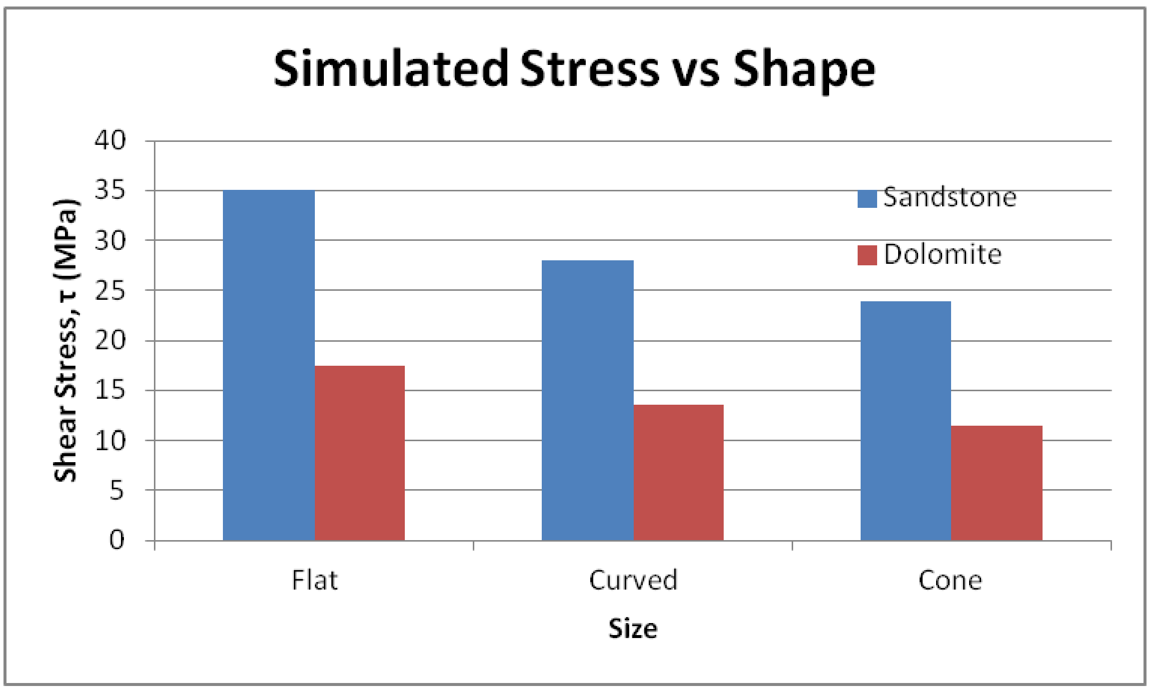

FIGURE 4.9: Effect on Shape of Cutter on Shear Stress (Simulation)

From the simulated result, the cutter with cone shape is best for the drilling application as it has the lowest stress compared to the other 2 shapes. This is because the shear contact area of cone shape cutter is the highest and with largest shear contact area, the least stress is exerted on the cutter. The result is good, as it tally with the equation findings with the analytical data and shows a same relationship. The result is then validated with the comparison between the simulated data and analytical data.

Table 4.14 shows the comparison between the simulation data and the analytical data.

TABLE 4.14: Stress Values for Different Shape of Cutter

	Sandstone Formation		**Dolomite Formation**	
Shape of Cutter	**Simulated Stress (MPa)**	**Analytical Stress (MPa)**	**Simulated Stress (MPa)**	**Analytical Stress (MPa)**
Flat	3.50E+07	2.76E+07	1.75E+07	1.44E+07
Curved	2.80E+07	2.54E+07	1.35E+07	1.32E+07
Cone	2.39E+07	1.99E+07	1.14E+07	1.03E+07

Figure 4.10 below shows the comparison between simulated stress and analytical stress for different shape of cutter.

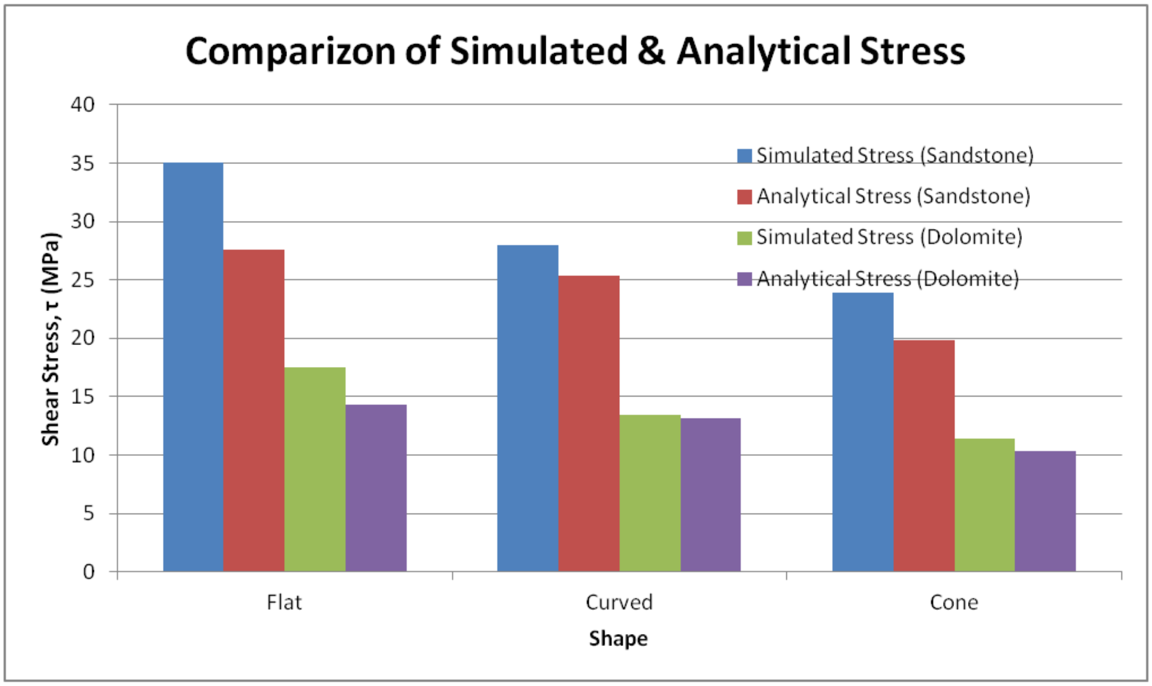

FIGURE 4.10: Comparison of Stress Values for Different Shape of Cutter

The von Mises stress obtained from the simulation data is higher than analytical data. This is due to the axial stress and not all forces are taken into the calculation of the analytical model. However, both the simulated and analytical stress data show the same behaviour, which tally with the theory based on the equation. Thus, both set of data show that the best shape of cutter for drilling operation in considerations of cutter durability is the cutter with cone shape.

4.2. PDC Cutter Wear

The wear of the cutter is calculated using the equation:

$$W = k_2 V \sigma^{\frac{1}{bn'}}$$

Parameters Used:

Proportionality constant,

$k_2 \times V = 1.5 \text{ x } 10^{-11}$,

Where k_2 is an arbitrary wear constant,

V is the deformed volume

$1/bn' = 6.45$,

where b is a constant whose value is approximately 0.5,

and n' is the cyclic strain-hardening coefficient which is equal to 0.31

From the equation, the von Mises stress is very dominant as it is going with a power of 6.45, while the other parameters are remained constant. The higher stress value will result in higher wear. The magnitude of the stress is dependent on the contact geometry, the mechanical properties of the materials, the friction and the externally applied forces.

4.2.1. Size of Cutter

The wear of the cutter with different size is shown in Table 4.15.

TABLE 4.15: Wear Values for different size of PDC cutter

Size of Cutter	Sandstone Formation		Dolomite Formation	
	Simulated Stress (MPa)	Simulated Wear (µm^2)	Simulated Stress (MPa)	Simulated Wear (µm^2)
8mm	9.25E+01	7.23E+01	4.65E+01	8.54E-01
13mm	4.30E+01	5.13E-01	2.16E+01	6.10E-03
16mm	3.50E+01	1.37E-01	1.75E+01	1.57E-03

Based on the Table 30, result shows that the cutter with size 16mm has the least wear compared to other size of cutter. PDC bit cutter with size 16mm has the lowest stress value and thus resulted in lowest wear.

4.2.2. Shape of Cutter

The wear value of the bit with different shape of cutter is shown in the Table 4.16.

TABLE 4.16: Wear Values for different shape of PDC cutter

Shape of Cutter	**Sandstone Formation**		**Dolomite Formation**	
	Simulated Stress (MPa)	**Simulated Wear (μm^2)**	**Simulated Stress (MPa)**	**Simulated Wear (μm^2)**
Flat	3.50E+01	1.37E-01	1.75E+01	1.57E-03
Curved	2.80E+01	3.23E-02	1.35E+01	2.92E-04
Cone	2.39E+01	1.16E-02	1.14E+01	9.98E-05

Based on the Table 31, cutter of cone shape has the least wear compared to flat and curved shape cutter. This is because cone shape cutter is with the largest shear contact area and least shear stress.

Chapter 5

Conclusion & Recommendation

5.1. Conclusion

Rate of penetration is important in optimizing the drilling performance, but by selecting suitable drill bit design which reduce the wear rate throughout the operation and increase the run length of the drill bit is another approach too. Most of the drilling operation is occurring at multi layer formation area which results in a more favorable choice to optimize the performance in run length rather than penetration rate. However, a maximize ROP is still favorable together with a suitable bit design for the multi layer formation operation area. Analytical model using the combination of both cutter-rock interaction model and Merchant's cutting model is formed to study the force and stress in the PDC cutter during drilling operation. Several bit design with different size and shape of cutter are simulated in ABAQUS and the best design which produce minimum wear rate during drilling operation is obtained. Results obtained that for this project, size of cutter with 16mm is best for cutter to increase the durability as the large shear contact area minimize the stress and lead to less wear compared to other size of cutter. As for the shape of cutter, cone shape is the best design to minimize wear and prolong the durability, as the same as the size of cutter, cone shape is with the largest shear contact area, which result in least stress and wear.

5.2. Recommendation

Due to the limitation of time and software, only simulation on the single cutter is done. The project can be improved using a better version of software and run the simulation for the whole bit instead of just on a single cutter. Further research can be made in the future to include other and more design features of the bit. Research on the other factors that would contribute to the bit wear rate can be explored too.

References

Bilgesu, H.I., Tetrick, L.T., Altmis, U., Mohaghegh, S., and Ameri, S., 1997. “A New Approach for the Prediction of Rate of Penetration (ROP) Values” *SPE Journal*.

Bit Technology, 2012. Baker Hughes Incorporated.

Cheatham, C.A. and Loeb, D.A.,1985. “Effect of Field Wear on PDC Bit Performance” *SPE/IADC Journal*.

Clayton, R., Chen, S., and Lefort, G., 2005. “New Bit Design, Cutter Technology Extend PDC Applications to Hard Rock Drilling” *SPE Journal*.

Drilling Engineering Workbook, 1995. Baker Hughes INTEQ

Glowka, D. A., 1987. *Development of a Method for Predicting the Performance and Wear of PDC Drill Bits*. Report SAND86-1745, Sandia Natl. Laboratories, New Mexico, UCS.

Glowka, D.A. and Stone, C.M.,1986. “Effects of Thermal and Mechanical Loading on PDC Bit Life” *SPE Journal*.

Fear, M.J., 1999. “How to Improve Rate of Penetration in Field Operations” SPE Journal **14 (1)**.

Muhammad Hariz, B.M.N., 2014. *Optimizing PDC Bit Design Features for Improvement in Rate of Penetration for Multi-layer Formation*. Universiti Teknologi PETRONAS, Perak, Malaysia.

Hareland, G., Yan, W., Nygaard, R., and Wise, J.L., 2009. “Cutting Efficiency of a Single PDC Cutter on Hard Rock” *Journal of Canadian Petroleum Technology*, **48 (6)**.

Henry, T., Corp, A., Sherif, M. and Ahmed Ragheb, 2011. “New PDC Technologies Increases Durability and Enables Fast Drilling in Hard Abrasive Formation” *SPE Jornal*.

IADC Dull Grading System for Fixed Cutter Bits and Roller Cone Bits, 2012. Baker Hughes Incorporated.

Introduction to PDC bits, 2002. Smith International Inc.

Jain, K.C. and Chitale, A.K., 2010. *Textbook of Production Engineering - Theory of Metal Cutting.* PHI Learning Private Limited, New Delhi.

Li, X.H. and Hood, M., 1993. “Wear and damage to PDC bits” *SPE Journal*.

Motahhari, H.R., 2008. *Improved Drilling Efficiency Technique Using Integrated PDM and PDC Bit Parameters*. University of Calgary, Calgary, Alberta.

Rajabov, V., Miska, S., Mortimer, L., Yu, M., and Ozbayoglu, E., 2012. “The Effects of Back Rake and Side Rake Angles on Mechanical Specific Energy of Single PDC Cutters with Selected Rocks at Varying Depth of Cuts and Confining Pressures” *SPE Journal*.

Tangena, A.G., 1990. *A Low Cycle Fatigue Wear Model and Its Application to Layered Systems.*

Tangena, A.G. and Wijhhoven P.J.M., 1988. *The Correlation between Mechanical Stresses and Wear in a Layered System.* Wear, 121 p. 27.

Warrwn, T.M. and Armegost, W.K., 1988. "Laboratory Drilling Performance of PDC Bits" *SPE Journal*.

Yahiaoui, M., Gerbaud, L. Paris, J-Y., Denape, J., and Dourfaye, A., 2012. *A Study on PDC Drill Bits Quality.* Ecole Nationale d'Ingénieurs de Tarbes, Tarbes, France.